

Modeling and experimental studies of carbon dioxide separation on zeolite fixed bed by cyclic pressure swing adsorption

Tomasz Aleksandrak*, Kamila Zabielska, Elżbieta Gabruś

West Pomeranian University of Technology in Szczecin, Faculty of Chemical Technology and Engineering, Department of Chemical and Process Engineering, Piastów 42, 71-065 Szczecin, Poland

*Corresponding author: e-mail: tomasz.aleksandrak@zut.edu.pl

The paper presents the results of experimental and model studies of the pressure swing adsorption (PSA) process in a column with a zeolite 13X bed with a height of 0.5 m. The gas mixture consisted of CO₂ (10–20%), N₂, and H₂O (RH 50%) in different ratios. As a result of the column tests, concentration, and temperature evolutions were obtained for each of the adsorption and desorption stages, which were used to determine the breakthrough and bed saturation times and other parameters important for the analysis of the column operation. A mathematical model of the PSA process for the separation of CO₂ from the gas mixture was developed. The system of second-order partial differential equations was solved using Matlab software. The research focuses on adsorptive CO₂ capture and shows the influence of water vapor and operational parameters on the quality of model validation.

Keywords: column adsorption, PSA, carbon dioxide, mathematical model, zeolite 13X.

INTRODUCTION

Flue gas streams emitted during fuel combustion or other technological processes contain numerous compounds that pollute the air, e.g. carbon dioxide, sulfur oxide, nitrogen oxides, methane, ozone, and freons. Carbon dioxide is the main greenhouse gas that causes global warming and is emitted into the atmosphere mainly in the processes of electricity and heat generation. One of the future methods of reducing CO₂ emissions into the atmosphere are separation processes based on adsorption¹.

In practice, adsorption is carried out in column apparatus and consists in passing gases through a fixed bed filled with a properly selected adsorbent. The process of adsorptive capturing of carbon dioxide from the gas mixture is usually carried out at elevated pressure because in this way the adsorption capacity of the adsorbent bed is significantly increased. Adsorbent regeneration is carried out in situ in adsorption-desorption installations operating cyclically in the PSA (Pressure Swing Adsorption) process. This technology is used in chemical and petrochemical processes as well as in metallurgy, for example for the recovery of hydrogen from coke oven or conversion gases. PSA can also be used to separate a mixture of gases, e.g. for obtaining oxygen and nitrogen from the air, separating methane or hydrocarbons, and drying gases. This process is characterized by low energy input and short cycle times. The development of this technology is aimed at obtaining a high concentration of CO₂ in the product with a high degree of recovery and at reducing the demand for the adsorbent and the energy necessary in the separation process. Thus, the separation of the gas mixture is possible due to kinetic effects and differences in adsorption equilibrium. The PSA process consists of four stages: compression, adsorption, expansion, and desorption^{2–5}.

The aim of the work is to extend the knowledge in the field of the cyclic PSA pressure swing adsorption process, applicable to the separation of difficult to adsorb gases, by example of CO₂ removal from streams containing nitrogen and water vapor.

EXPERIMENTAL

Experimental studies were performed for carbon dioxide, nitrogen, and water vapor. These compounds are the main components of the flue gas mixture and are often found in industry. The source of carbon dioxide (99.995%) and nitrogen (99.999%) were pressure gas cylinders (Messer, Poland), while the water came from the municipal water supply and was distilled before use.

The tests were performed on zeolite 13X (Hurtgral, Poland). Zeolite 13X is a reference material for CO₂ capture due to its unique structure, and resistance to high temperatures. The properties of the adsorbent are presented in Table 1.

Table 1. Physical Properties of Zeolite 13X^{6, 7}

Property	Zeolite 13X
Specific surface BET, m ² /g	700
Bulk density, kg/m ³	689
Grain diameter, m	0.003
Density, kg/m ³	1950
Apparent density, kg/m ³	1229
Pore radius, m	1 · 10 ⁻⁹
Grain porosity	0.37
Bed porosity	0.43
Specific heat, J/(kg · K)	920

The PSA pressure swing adsorption process was used to separate carbon dioxide from the model gas mixture. The installation of the cyclic PSA process (Fig. 1) consists of a thermally isolated stainless steel column with an internal diameter of 26 mm, an external diameter of 30 mm, and a length of 500 mm. The installation is equipped with 6 solenoid valves (VE1 – VE6) controlled by computer software.

The system is fitted with 2 control valves (VR1, VR2) to regulate the gas flow and a flow meter (MF). The accuracy of the flow setting is +/- 1%. A steam generator was used to generate the steam stream, which consists of a saturator made of acid-resistant steel with a capacity of about 200 ml. The saturator was placed in an AD07H200 water bath (PolyScience, USA). Gas flows are regulated by mass flow controllers MFC (Aalborg, USA), where the flow is regulated in the range of 0 ÷ 20 L/min for nitrogen and 0 ÷ 2 L/min for carbon dioxide.

The next element of the equipment is the pressure gauge (P) made of acid-proof steel. It is an absolute pressure gauge with a measurement range of 0÷1 MPa and an accuracy of 0.5%. Thermocouples (T_b , T_m , T_t) are connected to the column, which allows recording changes in gas temperature in the adsorbent bed. The thermocouples are located at 55, 250, and 450 mm from the bottom of the adsorption column.

For the analysis of gases in the installation, an analyzer based on the HPR-20 QIC (MS) quadrupole mass spectrometer (Hidden Analytical, UK) was used.

MATHEMATICAL MODELING

The cyclic PSA adsorption process consists of four stages: compression, adsorption from the model gas stream (model off-gas), exhaust, and bed regeneration (desorption). The work includes mathematical modeling of the following stages: adsorption and desorption. This approach is related to the fact that in the cyclic PSA process, the most important are the stages of adsorbent adsorption and regeneration, during which both mass and heat transfer take place.

When developing the mathematical model of the PSA process the following assumptions are made⁸:

- The flow pattern is described by a gas phase plug flow model with axial mass and heat dispersion;
- The gas phase obeys the ideal gas law;
- Pressure drop in the column is negligible;
- Gas velocity is constant;
- Radial temperature and concentration gradients are negligibly small;
- The mass transfer rate is represented by the linear model of the driving force (LDF);
- The isosteric heat of adsorption is constant;
- The adsorption isotherms of CO₂, N₂ and H₂O are described by the extended Langmuir model;

- There is no thermal equilibrium between the gas phase and the solid grains;

- Physical properties of the adsorbed substances and the walls of the adsorption column are independent of temperature and pressure.

According to the above assumptions the mathematical model consists of several partial differential equations (PDEs). The differential mass balance equation of component i in the gas phase in the PSA process is as follows⁹⁻¹¹:

$$-D_{axi} \frac{\partial^2 C_i}{\partial z^2} + w \frac{\partial C_i}{\partial z} + \frac{\partial C_i}{\partial t} + \frac{1 - \varepsilon_b}{\varepsilon_b} \rho_s \frac{\partial q_i}{\partial t} = 0 \quad (1)$$

The energy balance for the gas phase can be described by the following equation^{8, 9}:

$$-k_g \cdot \varepsilon_b \cdot \frac{\partial T_g}{\partial z^2} + C_{pg} \cdot w \cdot \rho_g \cdot \frac{\partial T_g}{\partial z} + \varepsilon_b \cdot C_{pg} \cdot \rho_g \cdot \frac{\partial T_g}{\partial t} + h \cdot a_p \cdot (T_g - T_s) + \frac{4 \cdot H_w}{D} (T_g - T_a) = 0 \quad (2)$$

The energy balance for the solid phase is presented by equation^{8, 9}:

$$-k_s \cdot \frac{\partial T_s}{\partial z^2} + C_{ps} \cdot \rho_s \cdot \frac{\partial T_s}{\partial t} + \rho_s \sum_{i=1}^{nc} (C_{ps} \cdot q_i) \frac{\partial T_s}{\partial t} + \rho_s \sum_{i=1}^{nc} (\Delta H_i \frac{\partial q_i}{\partial t}) - h \cdot a_p (T_g - T_s) = 0 \quad (3)$$

The adsorption rate was described by the linear driving force (LDF) model, which can be represented by the equation^{9, 12}:

$$\frac{\partial q_i}{\partial t} = k_i (q_i^* - q_i) \quad (4)$$

The LDF model is usually used to analyze the dynamics of an adsorption column and to design adsorption processes due to its simplicity and analytical consistency.

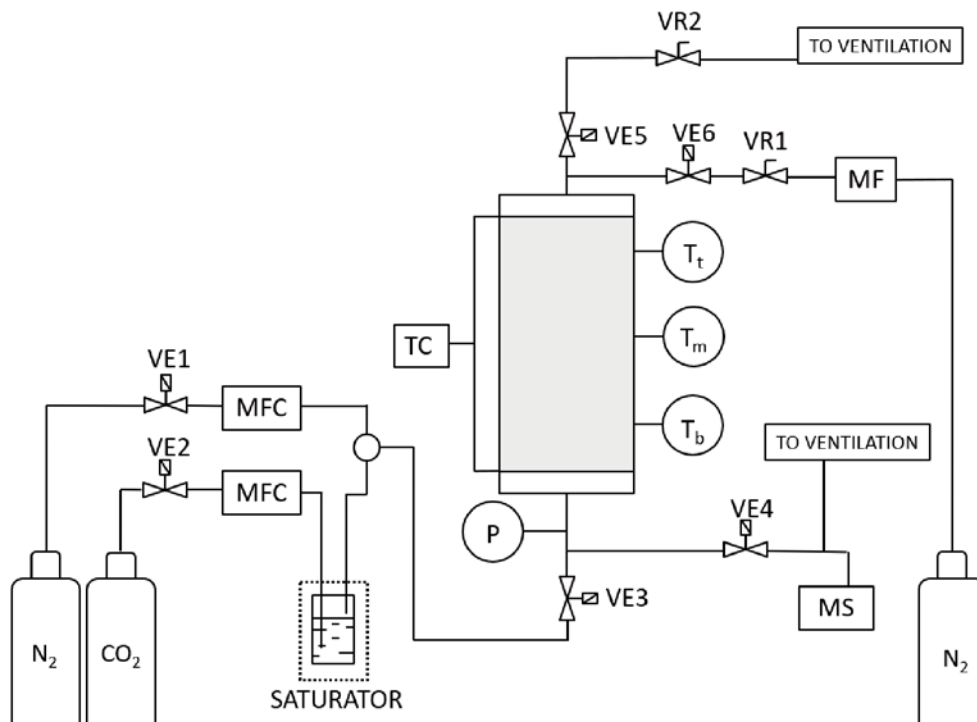


Figure 1. PSA installation diagram (VE – solenoid valve; MFC – mass flow controller; VR – manual control valve; MF – flow meter; P – pressure meter; T – thermocouple; MS – mass spectrometer, TC – temperature controller).

The equilibrium concentration of the component q_i^* is described by the extended Langmuir adsorption isotherm equation¹³:

$$q_i^* = \frac{A_{Li} \cdot \exp\left(\frac{B_{Li}}{T_s}\right) \cdot C_i \cdot R \cdot T_s}{1 + \sum_i C_{Li} \exp\left(\frac{D_{Li}}{T_s}\right) \cdot C_i \cdot R \cdot T_s} \quad (5)$$

The Langmuir isotherm model parameters obtained from own experimental measurements of adsorption equilibrium are presented in Table 2.

Table 2. Langmuir isotherm model parameters for N₂, CO₂, and H₂O on zeolite 13X

Parameter	CO ₂	N ₂	H ₂ O
A_L , mol/kg	0.00016	0.000002	0.7874
B_L , mol/kg·Pa	0.3238	-5.555	857.114
C_L , Pa ⁻¹	0.00003	0.0003	0.0001
D_L , K	0.5308	-2012.76	1720.554

The axial dispersion coefficient D_{ax_i} was calculated from the equation¹⁴:

$$D_{ax_i} = 0.73 \cdot D_{m_i} + \frac{w \cdot r_p}{\varepsilon_b \cdot \left(1 + 9.49 \frac{\varepsilon_b}{w \cdot d_p}\right)} \quad (6)$$

The axial dispersion coefficient does not affect the adsorption process in the gas phase to a large extent, but its use has a positive effect on the stability of numerical calculations.

The Fuller and Giddings equations were used to calculate the molecular diffusion coefficient¹⁵:

$$D_{m_i} = \frac{9.86 \cdot 10^{-5} \cdot T_g^{1.75}}{P \cdot (v_{d_i}^{1/3} + v_{d_j}^{1/3})^2} \left(\frac{1}{M_i} + \frac{1}{M_j}\right)^{1/2} \quad (7)$$

The mass transfer kinetic coefficient $k_{i,k}$ was calculated from equation^{8, 16}:

$$\frac{1}{k_i} = \frac{d_p}{6 \cdot k_{f_i}} + \frac{d_p^2}{60 \cdot \varepsilon_p \cdot k_{p_i}} \quad (8)$$

The resistance coefficient in the gas film surrounding the adsorbent grain k_{f_i} was calculated from the equation for the Sherwood number⁸:

$$k_{f_i} = \frac{Sh_i \cdot D_{m_i}}{d_p} \quad (9)$$

The diffusion coefficient in the pores of the adsorbent particle k_{p_i} was calculated on the basis of the equation^{8, 9}:

$$k_{p_i} = \tau \cdot \left(\frac{1}{D_{K_i}} + \frac{1}{D_{m_i}}\right) \quad (10)$$

The Knudsen diffusion coefficient D_{K_i} was defined as⁸:

$$D_{K_i} = 97 \cdot r_p \cdot \left(\frac{T_g}{M_i}\right)^{0.5} \quad (11)$$

The following equation was used to determine the heat transfer coefficient between the gas phase and the solid phase of the adsorbent⁸:

$$\alpha_k = j \cdot C_{pg} \cdot w \cdot \rho_g \cdot Pr \quad (12)$$

The value of the j_k coefficient depends on the Reynolds number⁸:

$$Re < 190 \quad j = 1.66 \cdot Re^{-0.51}$$

$$Re < 190 \quad j = 1.66 \cdot Re^{-0.51}$$

The Sherwood number is calculated from the following equation⁸:

$$Sh = 2 + 1.1 \cdot Sc^{1/3} \cdot Re^{0.6} \quad (13)$$

The Prandtl number was calculated from the following equation⁸:

$$Pr = \frac{\mu_g \cdot C_{pg}}{k_g \cdot M_g} \quad (14)$$

The Reynolds number is determined from the equation⁸:

$$Re = \frac{d_p \cdot \rho_g \cdot w}{\mu_g} \quad (15)$$

The thermal conductivity of the gas phase k_g was calculated from the equation using the analogy between heat conduction and mass diffusion⁸:

$$k_g = C_{pg} \cdot \sum_i (D_{ax_i} \cdot \gamma_i) \cdot \rho_g \quad (16)$$

The mathematical model was solved with the numerical method of lines (NMOL) in Matlab R2021b using the ODE23s solver function. The basic idea behind NMOL is to replace spatial derivatives in partial differential equations (PDEs) with algebraic approximations. Once this is done, spatial derivatives are no longer explicitly stated in terms of spatial independent variables. Then only the initial value variable remains, usually time in the physics problem. In other words, with only one independent variable left, we have a system of ordinary differential equations (ODE) that approximates the original PDE equation. The resulting ordinary differential equations can then be solved using numerical methods such as Runge-Kutta method. The NMOL is an efficient and effective method for obtaining accurate numerical results^{17, 18}.

The first-order partial derivatives were replaced by an upwind differencing scheme:

$$\frac{\partial \Gamma_j}{\partial z} = \frac{\Gamma_j - \Gamma_{j-1}}{\Delta z} \quad (17)$$

The second-order partial derivatives have been replaced by a central differencing scheme:

$$\frac{\partial^2 \Gamma_j}{\partial z^2} = \frac{\Gamma_{j+1} - 2 \cdot \Gamma_j + \Gamma_{j-1}}{\Delta z^2} \quad (18)$$

In the modeled system, a single-layer bed with a height of 0.50 m was divided into 30 nodal points. The distance between nodes is 0.017 m.

The presented general mathematical model of the cyclic PSA process should be solved for the appropriate boundary conditions. Accepted initial conditions and boundary values are presented in Table 3.

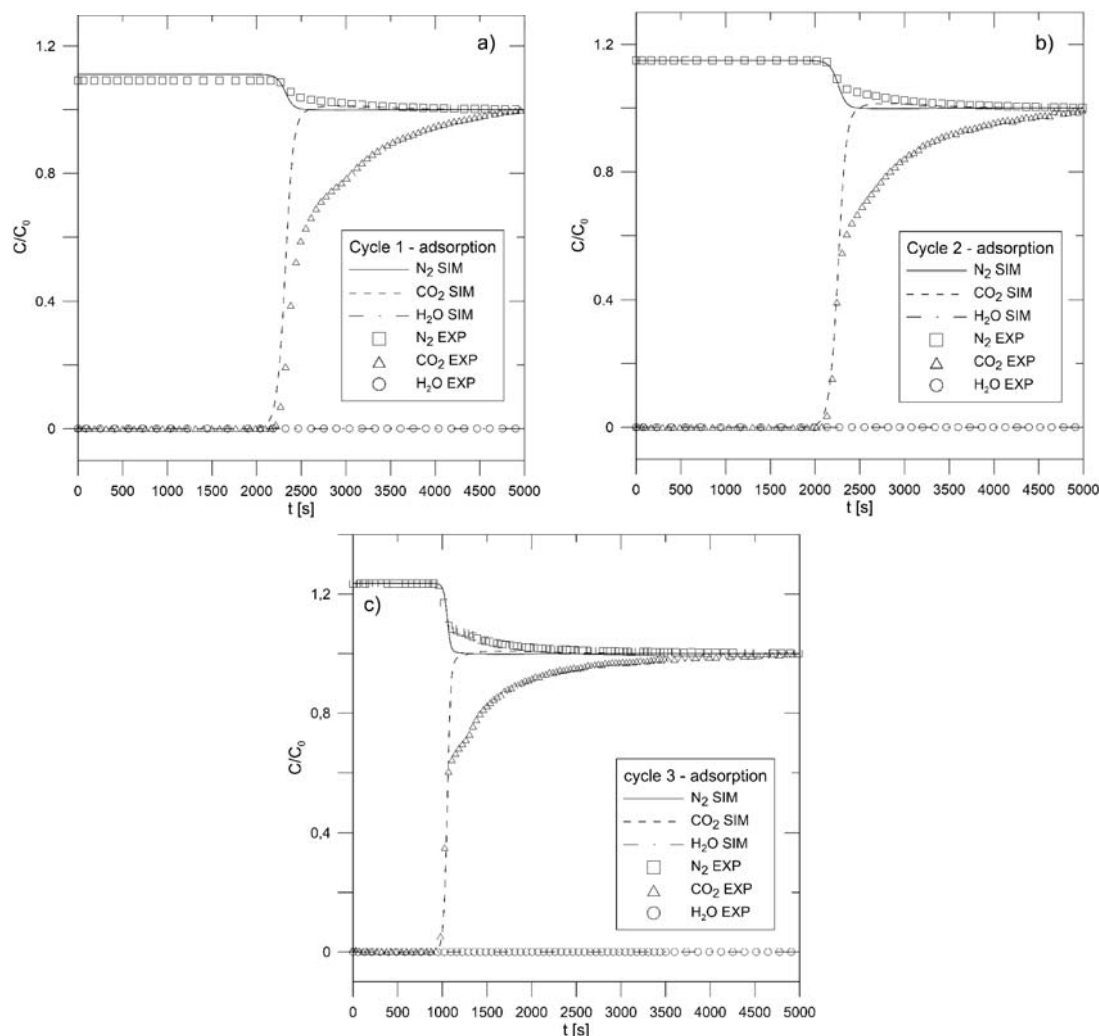
The conditions at the inlet to the column (gas phase temperature T_g , molar concentration C_i), had constant values throughout both the adsorption and desorption stages of the PSA process. The PSA process parameters are presented in Table 4.

Table 3. Initial and boundary conditions of the mathematical model of the cyclic PSA process

Cycle number	Composition	Inlet gas flow, L/min	RH, %	Ambient temperature, K	Pressure, MPa
1	N ₂ /CO ₂ /H ₂ O 89.99/10/0.01	1.78	50	323	0.3
2	N ₂ /CO ₂ /H ₂ O 84.98/15/0.02	1.80	50	326	0.3
3	N ₂ /CO ₂ /H ₂ O 79.98/20/0.02	2.0	50	330	0.3
4	N ₂ /CO ₂ /H ₂ O 89.99/10/0.01	1.78	50	323	0.5
5	N ₂ /CO ₂ /H ₂ O 84.98/15/0.02	1.80	50	326	0.5
6	N ₂ /CO ₂ /H ₂ O 79.98/20/0.02	2.0	50	330	0.5

Table 4. The PSA process parameters

Cycle No.	CO ₂ fraction	q _d mol/kg	q* mol/kg	t _{5%} s	t _{50%} s	t _{95%} s	φ	MTZ m	LUB m
0.3 MPa									
1	10%	1.72	2.34	1927	2093	3410	0.58	0.267	0.039
2	15%	1.86	2.61	1904	2037	3710	0.46	0.329	0.033
3	20%	2.06	3.05	977	1042	2245	0.31	0.462	0.031
0.5 MPa									
4	10%	1.99	2.71	2514	2656	3373	0.76	0.135	0.027
5	15%	2.22	3.18	2412	2530	3991	0.55	0.241	0.024
6	20%	2.38	3.48	1218	1285	2492	0.37	0.377	0.026

**Figure 2.** Experimental and simulated breakthrough curves for carbon dioxide, nitrogen, and water vapor in cycles 1 (a), 2 (b), and 3 (c)

RESULTS AND DISCUSSION

Measurements and simulations were carried out for a ternary mixture obtaining breakthrough curves for various concentrations of CO₂, N₂, and H₂O which are presented in Figures 2–3 for pressures of 0.3 and 0.5 MPa.

Based on the column tests, experimental and simulated temperature evolution (three control points) obtained for the adsorption stage of 15% carbon dioxide from the ternary mixture at pressures of 0.3 and 0.5 MPa are presented in Figure 4. The adsorption stage was

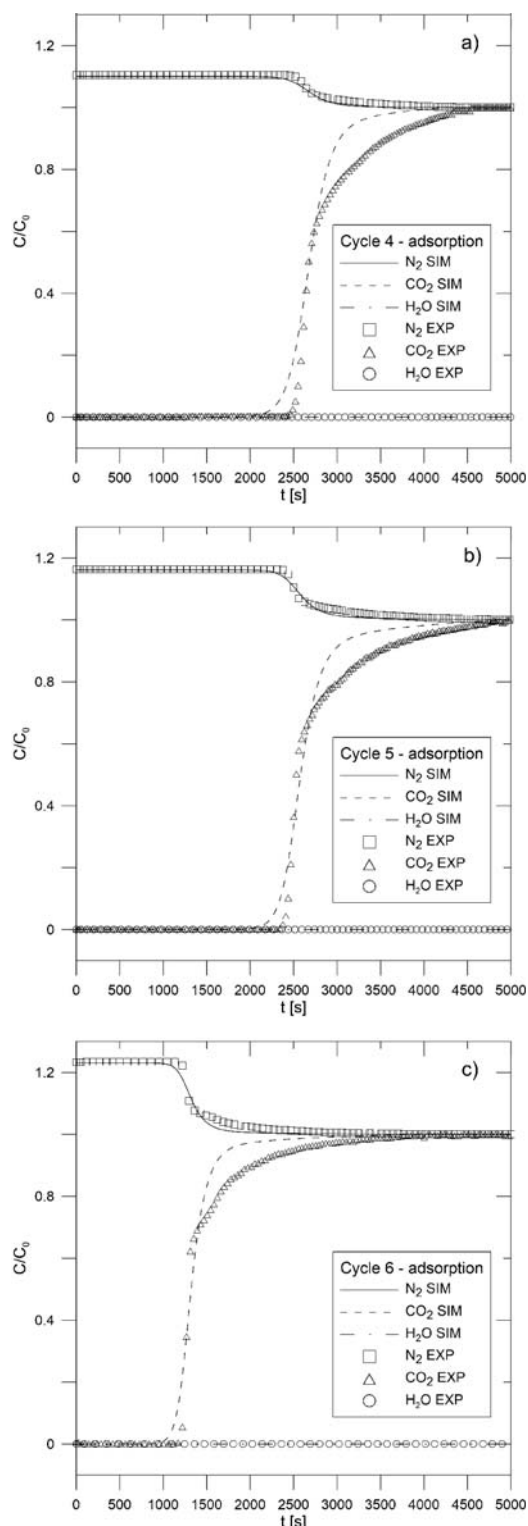


Figure 3. Experimental and simulated breakthrough curves for carbon dioxide, nitrogen, and water vapor in cycles 4 (a), 5 (b), and 6 (c)

followed by a blowdown and then a desorption step. The data for the desorption stage (breakthrough curves and temperature evolution) are presented in Figures 5–6. The desorption stage was conducted at atmospheric pressure.

The experimental breakdown curves (Fig. 2 and Fig. 3) show asymmetry. However, the results of the separation of ternary gas mixtures in the PSA adsorption stage are very well reproduced with model curves in almost the entire concentration range, in particular in the breakdown and stoichiometric regions.

Increasing the process pressure from 0.3 to 0.5 MPa increases the bed breakthrough time by about 20%,

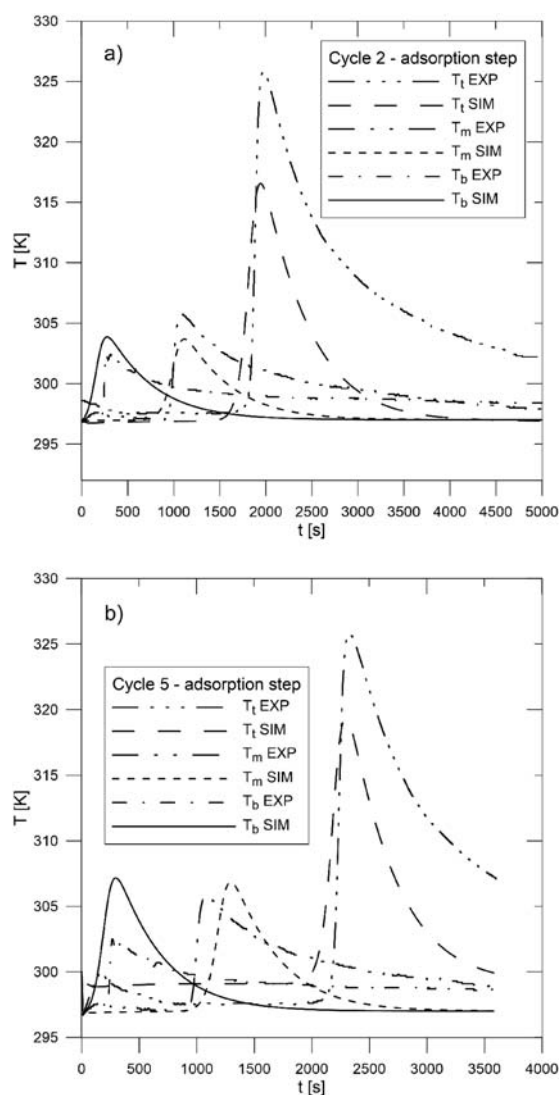


Figure 4. Experimental and simulated temperature evolution in the adsorption step in cycles 2 (a) and 5 (b)

which is beneficial due to the longer protection time of the adsorbent bed. Changes in concentration also cause changes in bed breakthrough time. An increase in the CO₂ concentration at the inlet to the column reduces the bed breakthrough time. For the 10% and 15% CO₂ fractions, the differences are small (2177 s and 2098 s for 0.5 MPa), while increasing the CO₂ fraction to 20% results in a significant decrease in the bed breakthrough time (1095 s for 0.5 MPa).

As can be seen in Fig. 4, the temperature evolution recorded during the adsorption stage shows a peak at the bed breakthrough, and the model accurately reflects its location moderately underestimating the temperature of the upper thermocouple.

The good agreement between the experimental and model desorption curves (Fig. 5) confirms the usefulness of the developed mathematical model for the PSA process and can be used to predict and simulate the process.

Figure 6 presents the experimental and model temperature evolution curves in the desorption stage, which confirms the good agreement between the profiles calculated from the mathematical model and obtained from the experiment.

Table 5 presents characteristic parameters such as: dynamic adsorption capacity q_d , actual adsorption capacity q^* , breakthrough times $t_{50\%}$, stoichiometric times $t_{50\%}$,

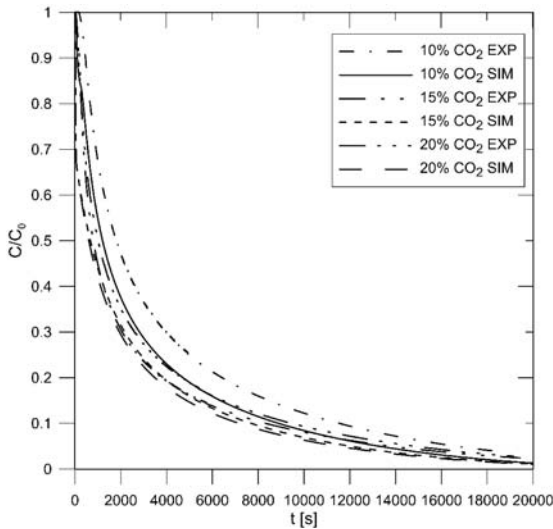


Figure 5. Experimental and simulated curves of the CO₂ desorption step on zeolite 13X at 0.1 MPa pressure

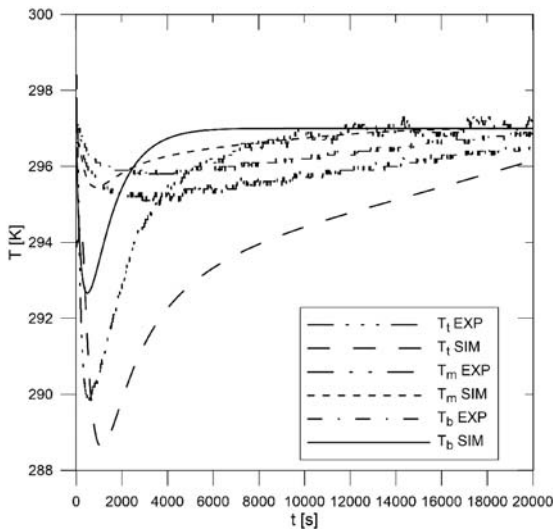


Figure 6. Experimental and simulated temperature evolution in the desorption step on zeolite 13X (15% CO₂, pressure 0.1 MPa)

Table 5. Characteristic parameters of the adsorption stage of the PSA process

Stage	Initial conditions	Boundary conditions
Adsorption	$C_{N_2}(z, 0) = P / (R \cdot T_g)$ $C_{CO_2}(z, 0) = 0$ $C_{H_2O}(z, 0) = 0$ $T_g(z, 0) = T_a$ $T_s(z, 0) = T_a$ $q_i(z, 0) = 0$	$C_i(0, t) = C_{i_0}$ $T_g(0, t) = T_a$ $T_s(0, t) = T_a$ $\frac{\partial C_i(L, t)}{\partial x} = 0$ $\frac{\partial T_g(L, t)}{\partial x} = 0$ $\frac{\partial T_s(L, t)}{\partial x} = 0$
Regeneration	$C_{N_2}(z, 0) = P / (R \cdot T_g)$ $C_{CO_2}(z, 0) = 0$ $C_{H_2O}(z, 0) = 0$ $T_g(z, 0) = T_a$ $T_s(z, 0) = T_a$ $q_i(z, 0) = q_i^*$	$C_i(0, t) = C_{i_0}$ $T_g(0, t) = T_a$ $T_s(0, t) = T_a$ $\frac{\partial C_i(L, t)}{\partial x} = 0$ $\frac{\partial T_g(L, t)}{\partial x} = 0$ $\frac{\partial T_s(L, t)}{\partial x} = 0$

saturation times $t_{0,95\%}$, symmetry factor for the output curve φ , the height of the mass transfer zone (*MTZ*) and length of the unused bed (*LUB*) in the adsorption stage of the PSA process.

The adsorption process takes place in the bed, at a certain height called the *MTZ* (Mass Transfer Zone). This zone moves towards the outlet of the adsorption column. In the case of practical application of adsorption, it is more advantageous when the shape of *MTZ* does not change along the entire length of the bed. The height of the *MTZ* mass exchange zone is the bed height at which the adsorbent concentration decreases from 95% to 5% of the initial concentration. This value can be calculated from the Michaels formula¹³:

$$MTZ = \frac{H(t_{0,95} - t_{0,05})}{t_{0,95} - (1 - \varphi)(t_{0,95} - t_{0,05})} \quad (19)$$

The efficiency of the adsorption column is greatly affected by the length of the *LUB* (Length of Unused Bed), which may occur as a result of the breakthrough process and incomplete saturation of the bed. It is better for the process if this value is as low as possible. Calculations of this relationship are based on experimental breakthrough curves and can be calculated based on the equation:

$$LUB = \left(1 - \frac{t_{0,05}}{t_{0,5}}\right) H \quad (20)$$

The symmetry factor φ can be calculated from the ratio of the area above the output curve to the total area above and below the output curve. The coefficient φ decreases with increasing concentration of carbon dioxide in the mixture, which increases the convexity of the breakdown curves. The height of the *MTZ* mass exchange zone increases with increasing CO₂ concentration. The *MTZ* height at 0.3 MPa is higher than that at 0.5 MPa for 3 different CO₂ concentrations and in three cases.

CONCLUSIONS

In many industrial processes, the exhaust gases released are characterized by a significant content of carbon dioxide and a certain level of humidity. The paper presents a theoretical and experimental analysis of the possibility of using the PSA process for the separation of carbon dioxide from a nitrogen stream in the presence of water vapor. According to the available literature data, the adsorption of carbon dioxide from the gas mixture in the presence of water is problematic. Theoretical predictions of the breakthrough curves based on the equilibrium data require experimental verification in the column installation, because the scientific publications to date show that water can limit the adsorption capacity of the adsorbent bed, but also increase the CO₂ capture rate or have the opposite effect.

Experimental studies of the PSA process were carried out in a wide range of process parameter variability. The results of the experiments were presented in the form of concentration breakthrough curves and temperature evolution, which were a picture of the operation of the adsorbent bed at individual stages of the PSA process and were used to verify the results of model calculations. The key adsorbate was CO₂, therefore the adsorption process was carried out each time until the bed was completely saturated, obtaining full breakthrough curves.

The investigation results indicate effective adsorption of CO₂ on zeolite 13X already at relatively low pressures (0.3 and 0.5 MPa), reaching the dynamic adsorption value

of about 70% of the equilibrium value. The length of the mass transfer zone *MTZ* is shorter than the bed height, which indicates efficient utilization of the adsorbent bed (low *LUB* value). The breakthrough time considered as the period of the adsorbent bed's protective action is sufficiently long, which is important from the point of view of the cyclic operation of the PSA installation.

A mathematical model was formulated, including all the mechanisms of mass and heat transport important for the PSA process, as well as assumptions regarding the individual stages of the process in accordance with the analysis of own experimental data. The developed model consisted of partial differential equations of the mass and energy balance together with equations describing the transport rate and adsorption equilibrium as well as boundary conditions enabling its solution. The developed and verified model of the cyclic process of pressure swing adsorption (PSA) predicts well the concentration bed breakthrough curves and the temperature evolution in the column in the adsorption stage, but also the concentration and temperature evolution in the desorption stage. The mathematical model can be useful for the purposes of designing and optimizing the cyclic PSA process applicable to the separation of gases from a mixture.

SYMBOL DESCRIPTION

A_L	– Langmuir isotherm parameter, mol/kg
a_p	– specific particle surface per unit volume bed, 1/m
B_L	– Langmuir isotherm parameter, K
C	– molar concentration, mol/m ³
C_L	– Langmuir isotherm parameter, –
C_{pg}	– specific gas phase heat capacity at constant pressure, J/mol · K
C_{ps}	– specific heat capacity of the adsorbent., J/kg · K
D	– internal diameter of the adsorption column, m
D_{ax}	– axial dispersion coefficient, m ² /s
D_L	– Langmuir isotherm parameter, K
D_K	– Knudsen diffusion coefficient, m ² /s
D_m	– molecular diffusion coefficient, m ² /s
d_p	– diameter of the adsorbent grain, m
h	– gas-solid heat transfer coefficient, W/m ² · K
H_w	– gas-wall heat transfer coefficient, J/m ² · s
j	– factor for heat or mass transfer, -
k	– mass transfer coefficient, 1/s
k_g	– gas phase thermal conductivity, W/m · K
k_f	– film mass transfer coefficient, m/s
k_p	– pore diffusivity, m ² /s
k_s	– adsorbent thermal conductivity, W/m · K
L	– height of the adsorbent bed, m
M	– molecular weight, kg/mol
M	– molecular weight of gas phase, kg/mol
p	– pressure, Pa
Pr	– Prandtl number, -
q	– adsorbed phase concentration, mol/kg
q^*	– equilibrium adsorbed phase concentration, mol/kg
R	– ideal gas law constant, J/mol · K
r_p	– dsorbent radius, m
Re	– Reynolds number, -
Sc	– Schmidt number, -
Sh	– Sherwood number, -
t	– time, s

T_a	– ambient temperature, K
T_g	– gas temperature, K
T_s	– adsorbent temperature, K
w	– superficial gas velocity, m/s
y	– mole fraction, mol/mol
z	– axial coordinate in the bed, m

Greek letters

α_k	– heat transfer coefficient, W/m ² · K
ΔH	– heat of adsorption, J/mol
ε_b	– bed porosity, m ³ /m ³
ε_p	– adsorbent grain porosity, m ³ /m ³
μ_g	– dynamic viscosity of gas phase, Pa · s
ρ_g	– gas density, kg/m ³
ρ_s	– adsorbent bulk density, kg/m ³
τ	– tortuosity factor, -

Subscripts

i	– component i
j	– component j

LITERATURE CITED

- Lin, C.-C., Liu, W.-T. & Tan C.-S. (2003). Removal of carbon dioxide by adsorption in a rotating packed bed. *Ind. Eng. Chem. Res.* 42, 2381–2386. DOI: 10.1021/ie020669+.
- Ben-Mansour, R., Habib, M.A., Bamidele, O.E., Basha, M., Qasem, N.A.A., Peedikakkal, A., Laoui, T. & Ali, M. (2016). Carbon capture by physical adsorption: Materials, experimental investigations and numerical modeling and simulations – A review. *Appl. Energy* 161, 225–255. DOI: 10.1016/j.apenergy.2015.10.011.
- Chao, C., Deng, Y., Dewil, R., Baeyens, J. & Fan, X. (2021). Post-combustion carbon capture. *Renew. Sust. Energ. Rev.* 138, 110490. DOI: 10.1016/j.rser.2020.110490.
- Raganati, F., Miccio, F. & Ammendola, P. (2021). Adsorption of Carbon Dioxide for Post-combustion Capture: A Review. *Energy Fuels* 35, 12845–12868. DOI: 10.1021/acs.energyfuels.1c01618.
- Siqueiraa, R.M., Freitas, G.R., Peixotoa, H.R., Nascimento, J.F., Musseb, A.P.S., Torres, A.E.B., Azevedoa, D.C.S. & Bastos-Netoa, B. (2017). Carbon dioxide capture by pressure swing adsorption. *Energy Procedia* 114, 2182–2192.
- Maring, B.J. & Webley, P.A. (2013). A new simplified pressure/vacuum swing adsorption model for rapid adsorbent screening for CO₂ capture applications. *Int. J. Greenh. Gas Con.* 15, 16–31. DOI: 10.1016/j.ijggc.2013.01.009.
- Zabielska, K., Aleksandrak, T. & Gabruś, E. (2020). Influence of humidity on carbon dioxide adsorption on zeolite 13X. *Chem. Eng. Process* 41, 197–208. DOI: 10.24425/cpe.2020.132542.
- Qazvini, O.T. & Fatemi, S. (2015). Modeling and simulation pressure-temperature swing adsorption process to remove mercaptan from humid natural gas; a commercial case study. *Sep. Purif. Technol.* 139, 88–103. DOI: 10.1016/j.seppur.2014.09.031.
- Gholami, M., Talaie, M.R. & Aghamiri, S.F. (2016). The development of a new LDF mass transfer correlation for adsorption on fixed beds. *Adsorption* 22, 195–203. DOI: 10.1007/s10450-015-9730-4.
- Li, S., Deng, S., Zhao, L., Zhao, R., Lin, M., Du, Y. & Lian, Y., (2018). Mathematical modeling and numerical investigation of carbon capture by adsorption: Literature review and case study. *Appl. Energy* 221, 437–449. DOI: 10.1016/j.apenergy.2018.03.093.
- Song, C., Kansha, Y., Fu, Q., Ishizuka, M. & Tsutsumi, A. (2016). Reducing energy consumption of advanced PTSA CO₂

capture process – Experimental and numerical study. *J. Taiwan Inst. Chem. Eng.* 64, 69–78. DOI: 10.1016/j.jtice.2015.12.006.

12. Mulgundmath, V.P., Jones, R.A., Tezel, F.H. & Thibault, J. (2012). Fixed bed adsorption for the removal of carbon dioxide from nitrogen: Breakthrough behaviour and modelling for heat and mass transfer. *J. Sep. Purif.* 85, 17–27. DOI: 10.1016/j.seppur.2011.07.038.

13. Thomas, W.J. & Crittenden, B. (1998). Adsorption Technology and Design. Butterworth-Heinemann.

14. Chou, C.-T. & Chen, C.-Y. (2004). Carbon dioxide recovery by vacuum swing adsorption. *J. Sep. Purif.* 39, 51–65. DOI: 10.1016/j.seppur.2003.12.009.

15. Fuller, E.N., Schettler, P.D. & Giddings, J.C. (1966). New method for prediction of binary gas-phase diffusion coefficients. *Ind. Eng. Chem.* 58(5), 18–27. DOI: 10.1021/ie50677a007.

16. Ruthven, D.M., Farooq, S. & Knaebel, K.S. (1994). Pressure Swing Adsorption, VCH Publishers.

17. Hamdi, S., Schiesser, W. & Griffiths, G.W. (2007). Method of lines, Scholarpedia.

18. Schiesser, W.E. & Griffiths, G.W. (2009). A compendium of partial differential equation models. Method of Lines Analysis with Matlab. Cambridge University Press, DOI: 10.1017/CBO9780511576270.